Inverse Problems, Design and Optimization Symposium
Rio de Janeiro, Brazil, 2004

Electrical Impedance Ground Prospecting for Anomaly Detection using Direct Inversion Algorithm with Dual Reciprocity Boundary Element Modeling

Y. Kagawa, W. Xu*, Y. Zhao, N. Wakatsuki and H. Totsuji*

Department of Electronics and Information Systems,
Akita Prefectural University, Honjo, Akita, 015–0055, Japan

1 Abstract

Anomaly detection is a technique to visualize the interior from the impedance data measured on the ground surface for geophysical applications from the oil field prospecting to the land mine searching. We have developed the direct inversion algorithm for the electrical impedance tomography based on the dual reciprocity boundary element modeling, first for the two-dimensional field and then for the three-dimensional field problems. The validation has been made for the cases when the impedance data are available for the electrical current emanation diagonally injected to the surface surrounding the field of interest [1, 2]. In practical prospecting, however, this is not always the case, in which the data are only accessible on the ground surface. Present paper demonstrates with some examples that the anomaly detection is possible though the resolution is poor.

2 Introduction

Anomaly detection is an important area of geophysical sensing, from oil field to land mine searching. This is a technique to visualize the interior from the impedance data remotely sensed over the surface. The electrical impedance sensing is one of the oldest techniques for geophysical exploration and yet plays an important role among others as it only requires a relatively inexpensive apparatus. This is widely practiced [3–5], in which the theory is based on the assumption like an X-ray tomography so that the practical applications are limited. It was attempted with the impedance data for the diagonal current injection which were possible with the boreholes drilled deep into the ground [6]. There is another field of application for medical care and monitoring [7].

The final goal is to achieve the imaging of the body interior. For experimental purpose, Barber and Brown [8, 9] developed the apparatus called APT (applied potential tomography), which was once commercially available. The image reconstruction uses the backprojection algorithm similar to the X-ray computed tomography in which the currents are assumed to flow in straight between a pair of the current electrodes. Barber and Brown also used a direct inversion approach, in which the currents between the injection current electrodes are partially considered to bend but the diffusive nature of the current was ignored. Generally, this does not apply, and the currents flow through multipaths. Therefore, in most inversion, iterative approach is used. Equations must be established to satisfy the Ohm's law for the line integral for each assumed path. The direct inversion is thus not possible. Instead, the resistivity distribu-

*Okayama University, Okayama, Japan

tion is iteratively modified so as to minimize the error function defined as the norm between the potentials observed for a certain current injection and the potentials evaluated for the above equations for the assumed resistivity distribution chosen as design variables.

We successfully developed the direct inversion algorithm for the electrical impedance tomography based on the dual reciprocity boundary element models in two dimensions [1].The modeling and algorithm were extended to the three dimensional field , for which the cases when the boreholes are provided to obtain the impedance data for the diagonal current injection were examined [2]. The injecting conditions are all similar to the so-called opposite method [7]. Here we demonstrate the cases when the data are only accessible on the ground surface. This condition is somewhat similar to the so-called neighboring method [7]. Many electrical impedance imagings only consider the cross-section of the field or two dimensional plane, in which the current flow is assumed to stay within the plane of reference. This is not true, as the current field is diffusive, the current paths will be out of the plane, which should not be ignored. Therefore, the three dimensional modeling is essential.

3 Field and Boundary Element Modeling

3.1 Nonhomogeneous Field Expression

The aim of the present study is to visualize the conductivity distribution from the data collected between the electrodes placed on the ground surface. The cross-sectional view is depicted in Fig. 1. The currents do not much flow outside of a cubic region indicated by dotted lines, in which an anomaly is buried. This region is only considered for the analysis with proper boundary conditions imposed without loosing the generality. The nonhomogeneous space is governed by the Laplace equation

$$\nabla \cdot (\sigma \nabla \psi) = 0 \tag{1}$$

with boundary conditions

$$\begin{aligned} \psi &= \hat{\psi}_i && \text{on the electrodes} \\ p &= \frac{\partial \psi}{\partial n} = \hat{p} && \text{over the boundary} \end{aligned} \tag{2}$$

where ψ is the potential, p is its normal derivative or flux and σ is the conductivity depending on the spatial position $\sigma = \sigma(x, y, z)$. It should be noted that for homogeneous field when σ is constant, eq.(1) is

$$\nabla^2 \psi = 0 \tag{3}$$

When the field is not homogeneous, eq.(1) can be transformed into a Poisson equation as

$$\nabla^2 \psi = b \tag{4}$$

where

$$\begin{aligned} b &= -\frac{1}{\sigma} \nabla \sigma \cdot \nabla \psi \\ &= \frac{1}{\sigma} \left(\frac{\partial \sigma}{\partial x} \frac{\partial \psi}{\partial x} + \frac{\partial \sigma}{\partial y} \frac{\partial \psi}{\partial y} + \frac{\partial \sigma}{\partial z} \frac{\partial \psi}{\partial z} \right) \end{aligned} \tag{5}$$

Thus the Laplace equation for the nonhomogeneous field is transformed into the Poisson-type expression with the distributed forcing term. Eq.(5) shows that when the distributions of b and $\nabla \psi$ are known, the distribution of σ can be obtained.

3.2 Dual Reciprocity in Charge Simulation Method

Dual reciprocity method (DRM) was first introduced to the boundary element solution of elastic field problems by Nardini and Brebbia [10]. The boundary element solution of Poisson equation involves the domain integral in association with the forcing term. The presence of the inhomogeneous term destroys the merit of dealing with the boundary only in boundary element method. The

DRM is a relief of the symtom, which removes the domain integral at the expense of the introduction of the particular solutions. The procedure is exactly the same as that in ref. [1] except that the problem is now three dimensional [2]. The solution of eq.(4) can be expressed as a linear combination of the general solution of the homogeneous Laplace equation and the particular solution of the inhomogeneous Poisson equation, so that

$$\psi = \varphi + \phi \tag{6}$$

where φ is the fundamental solution of $\nabla^2\varphi = 0$ and ϕ is the particular solution of $\nabla^2\phi = b$. Substituting eq.(6) into eqs.(4) and(5), one obtains the equation

$$\nabla^2\phi = 0 \tag{7}$$

with the boundary conditions

$$\begin{aligned} \phi =& \hat{\phi}_i = \hat{\psi}_i - \varphi_i \quad \text{on the electrode } i \\ \frac{\partial\phi}{\partial n} =& \hat{p} - \frac{\partial\varphi}{\partial n} \qquad \text{on the boundary} \end{aligned} \tag{8}$$

Eq.(7) is the Laplace equation and the boundary element discretization leads to the linear algbraic expression of standard form

$$[K]\{\phi\} - [G]\left\{\frac{\partial\phi}{\partial n}\right\} = 0 \tag{9}$$

where $[K]$ and $[G]$ are a system and its companion matrices, and $\{\phi\}$ and $\{\frac{\partial\phi}{\partial n}\}$ are the potential and its normal derivative or flux vectors associated with the nodes on the boundary. The boundary surface is divided into M elements, for which N boundary nodes and L internal points are considered. The potential ψ_i at an arbitrary point i can be expanded as

$$\begin{aligned} \psi_i &= \sum_{\ell=1}^{N+L} \varphi^*_{i\ell}\alpha_\ell + \sum_{j=1}^{M} \phi^*_{ij}\beta_j \\ &= \{\varphi^*\}_i^T\{\alpha\} + \{\phi^*\}_i^T\{\beta\} \end{aligned} \tag{10}$$

ϕ^*_{ij} is the fundamental solution of the homogeneous equation $\nabla^2\phi = 0$, which is evaluated at point i for a unit source excitation at point j on the boundary ($j = 1, 2, \ldots, M$). Coefficient β_j therefore corresponds to the fictitious charge associated with the boundary element j. $\varphi^*_{i\ell}$ is the particular solution of the Poisson equation

$$\nabla^2\varphi_{i\ell} = f_{i\ell} \tag{11}$$

The essence of the DRM lies in the expansion of the forcing term in terms of the approximate function $f_{i\ell}$ arbitrary chosen, so that

$$\begin{aligned} b_i = \sum_{\ell=1}^{N+L} f_{i\ell}\alpha_\ell = \sum_{\ell=1}^{N+L} (\nabla^2\varphi^*_{i\ell})\alpha_\ell \\ (\ell = 1, 2, \ldots, N+L) \end{aligned} \tag{12}$$

In matrix form,

$$\{b\} = [F]\{\alpha\} \quad \text{or} \quad \{\alpha\} = [F]^{-1}\{b\} \tag{12'}$$

where $F_{i\ell} = f_{i\ell}$. After ref. [10], the approximate function is here chosen to be

$$f_{i\ell} = 1 + r_{i\ell} \qquad \text{or} \qquad f_{i\ell} = \frac{r_{i\ell}}{r_{\max}} \tag{13}$$

where $r_{i\ell}$ is the distance between the source point i and the point of consideration ℓ, and $r_{\max}$ is the maximum distance. The particular solution that satisfies eq.(11) is

$$\varphi^*_{i\ell} = \frac{1}{12 r_{\max}} r^3_{i\ell} \tag{14}$$

when the second function of eq.(13) is used. Eq.(14) is different from the expression for the two dimensional case [1].

The surface is divided into triangular surface elements and the nodes are taken at the element corners and the fictitious or simulated charges are placed at the centers, which are shown in Fig. 2.

The fundamental solution of the homogeneous equation is

$$\phi^*_{ij} = \frac{1}{4\pi r_{ij}} \tag{15}$$

where r_{ij} is the distance between two points i and j, that is

$$r_{ij} = \sqrt{X^2 + Y^2 + Z^2}$$

where

$X = x_i - x_j$, $Y = y_i - y_j$ and $Z = z_i - z_j$

which is also different from the one for the two dimensional. Coefficient β_j corresponds to the magnitude of the fictitious charge placed at point j. Eqs.(8)and(12′) are substituted into eq.(9) and the discretized equation for the Poisson equation is obtained as follows, in the end.

$$\{\psi\} - [G]\left\{\frac{\partial\psi}{\partial n}\right\} = ([K][H] - [G][Q])\{\alpha\} \tag{16}$$

where

$$[K] = [E]([G]^{-1})^T[U] \tag{17}$$

and

$$\{\beta\} = ([G]^{-1})^T[U]\{\phi\} \tag{18}$$

The definition of the components of the matrices is the same as those in ref. [2], which are

$$\begin{aligned} E_{ij} =& \frac{1}{2}\sum_{m=1}^{M}\int_{\Gamma_m}\phi^*_{im}\frac{\partial\phi^*_{jm}}{\partial n}d\Gamma_m \\ &+ \frac{1}{2}\sum_{m=1}^{M}\int_{\Gamma_m}\phi^*_{jm}\frac{\partial\phi^*_{im}}{\partial n}d\Gamma_m \end{aligned} \tag{19}$$

$$\begin{aligned} G_{ij} &= \int_{r_j}\phi^*_{ij}d\Gamma_j \\ H_{ij} &= \varphi^*_{i\ell} \\ Q_{i\ell} &= \frac{\partial\varphi^*_{i\ell}}{\partial n} = q^*_{i\ell} \end{aligned} \tag{20}$$

$$(\ell = 1, 2, \ldots, N+L)$$
$$(i, j = 1, 2, \ldots, M)$$

and, when the constant elements are used,

$$\begin{aligned} U_{ij} &= \text{the area of element } j \quad (i = j) \\ U_{ij} &= 0 \qquad\qquad\qquad\quad (i \neq j) \end{aligned} \tag{21}$$

3.3 Direct Inversion

Eq.(16) are solved for $\{\alpha\}$, that is, $\{b\}$ with eq.(12′), under the boundary conditions and the potential data $\{\psi\}$ "measured" on the boundary, for the boundary condition $\{\frac{\partial\psi}{\partial n}\}$ when the current is injected between a pair of the electrodes chosen. Eq.(5) can be written as

$$\begin{aligned} &\nabla R_i \cdot \nabla\psi_i \\ &= \left(\frac{\partial R_i}{\partial x}\right)\frac{\partial\psi_i}{\partial x} + \left(\frac{\partial R_i}{\partial y}\right)\frac{\partial\psi_i}{\partial y} + \left(\frac{\partial R_i}{\partial z}\right)\frac{\partial\psi_i}{\partial z} \\ &= b_i^{(k)} \end{aligned} \tag{22}$$

where R is the logarithmic resistivity coefficient $R_i = -\ell_n\sigma_i$, $(\sigma_i = \sigma(x_i, y_i, z_i))$ and $\frac{\partial R_i}{\partial x}$ is the slope of R in x-direction about point i. $\psi_i = \psi(x_i, y_i.z_i)$ is the potential at point i and $\frac{\partial\psi_i}{\partial x}$ is the potential gradient in x-direction about point i in the domain. The potential ψ_i and its gradients $\frac{\partial\psi_i}{\partial x}, \frac{\partial\psi_i}{\partial y}$ and $\frac{\partial\psi_i}{\partial z}$ in the arbitrary point i are evaluated by eq.(10) as $\{\alpha\}$ and $\{\beta\}$ (eq.(18)) are now known. The three slopes of the logarithmic resistivity coefficient are unknowns in eq.(22). One has three equations of the form of eq.(22) for the three times of "the measurements" with different current injection ($k = 1, 2\ and\ 3$), which can be solved for the unknowns.

When the field is isotropic and the slope is the same for each direction, or $\frac{\partial R}{\partial x} = \frac{\partial R}{\partial y} = \frac{\partial R}{\partial z}$, the solution is theoretically obtained to the data for a single measurement. In practical situation, we establish as many equations for the measured potential data as the times of injection. These simultaneous equations are over-determined, which are however solved in the least square sense.

4 Numerical Demonstration

For the test case, a region closed by a dotted lines, depicted in Fig. 1, is taken. A cubic field ($10^3\mathrm{m}^3$) as shown in Fig. 2 is considered for simulation. The surfaces are divided into the triangular elements and the electrodes are placed only on the top surface (which corresponds to a part of the ground surface). As the current is supplied between a pair of the electrodes, the currents leaking out into the outer region will be very small. The natural boundary condition is thus set except on the electrodes. The case when there

placed is a cubic anomaly (2^3 m^3, conductivity is 10% higher) is buried in the middle. The logarithmic resistivity coefficient could be obtained by integrating the solutions $\frac{\partial R_i}{\partial x}$, $\frac{\partial R_i}{\partial y}$ and $\frac{\partial R_i}{\partial z}$ for a cubic pixel i along x, y and z directions. For the "measured" data, the solution of the forward problem is used. Fig. 3(a) shows the distribution of the relative conductivity distribution thus inverted. The simultaneous equations are formed for the injections of every possible pairs of electrode combination.

5 Concluding Remarks

The direct inversion algorithm for the three dimensional prospecting was proposed and the numerical simulation was extended to the case when the data are accessible only on the ground surface. The method proposed was successful. The demonstration shows that the inverted distribution is capable of identifying the position of an anomaly but the distribution resoution is not so clear as in the case when the data are available over the additional surfaces surrounding the region of inspection with the boreholes provided down into the ground [2].

The purpose of the present paper is to confirm the capability of the anomaly detection from the data only obtained over the ground surface. No further consideration such as the minimum number of the electrodes, sensitivity analysis, are included. Computation time required for the inversion is of the order of a few hours on PC.

References

[1] Y. Kagawa, Y. Sun and Y. Zhao: Direct inversion algorithm for electrical impedance tomography using dual reciprocity boundary element models, *Inverse Problems in Engineering*, **15** pp 217–237 (1997)

[2] T. Horikane, T. Hataya, W. Xu, Y. Zhao and Y. Kagawa: 3D electrical impedance prospecting simulation based on dual reciprocity boundary element modelling, *Inverse Problems in Engineering Mechanics III*, M. Tanaka, G. S. Dulikravich Ed., *Elsevier Science* pp 411–418 (2002)

[3] H. Shima, K. Kajima and H. Kamiya: Resistisity Image Profiling, *Kokin-Shoin, Tokyo* (1995), in Japanese

[4] A. Apporas :Developments in Geoelectrical Methods, *A.A.Balkema Pub., Rotterdam* (1997)

[5] H. P. Patra and S. K. Nath : Schlumberger Geoelectric Sounding in Ground Water, Principles, Interpretation and Application, *A.A.Balkema Pub., Rotterdam* (1999)

[6] K. A. Dines and J. R. Lytle : Computerized geophysical tomography, *Proc. IEEE*, **67**, 7 pp 1065–1093 (1979)

[7] J. W. Webster ed. : Electrical Impedance Tomography, *Adam Hilger Series on Biomedical Engineering, Adam Hilger, Bristol* (1990)

[8] D. C. Barber and B. H. Brown: Imaging spatial distributions of resistivity using applied potential tomography, *Elect. Lett. 19*, pp 933–935 (1983)

[9] B. H. Brown, D. C. Barber and A. D. Seagar: Applied potential tomography: Clinical possible applications, *Clin. Phys. Physiol. Meas.*, pp 109–121 (1985)

[10] P. W. Partridge, C. A. Brebbia and L. C. Wrobel: The Dual Reciprocity Boundary Element Method, *Computational Mechanics, Southermpton* (1992)

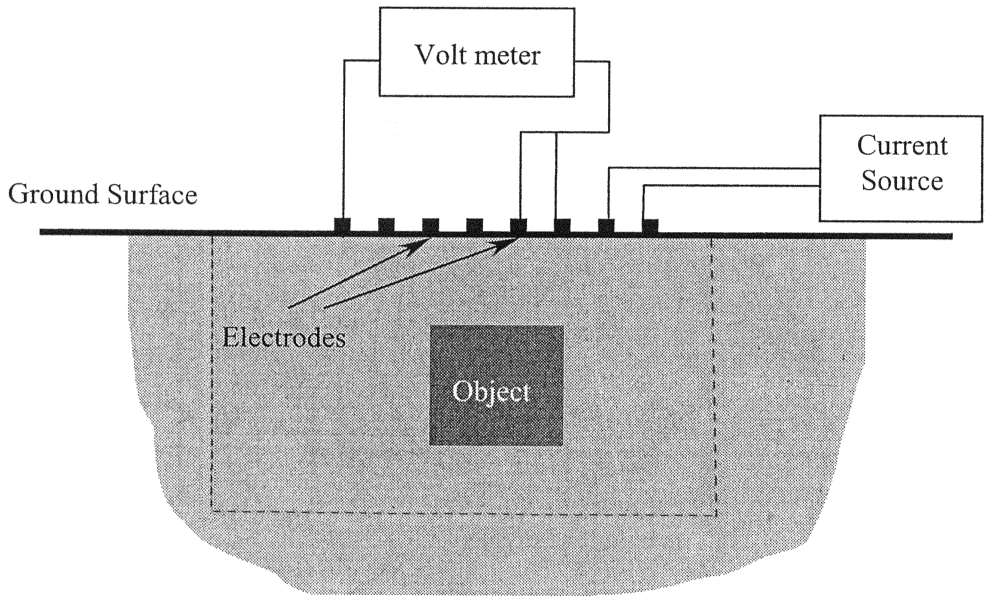

The data is collected only from the electrodes arrayed on the ground surface

Fig. 1: Field and electrode arrangement

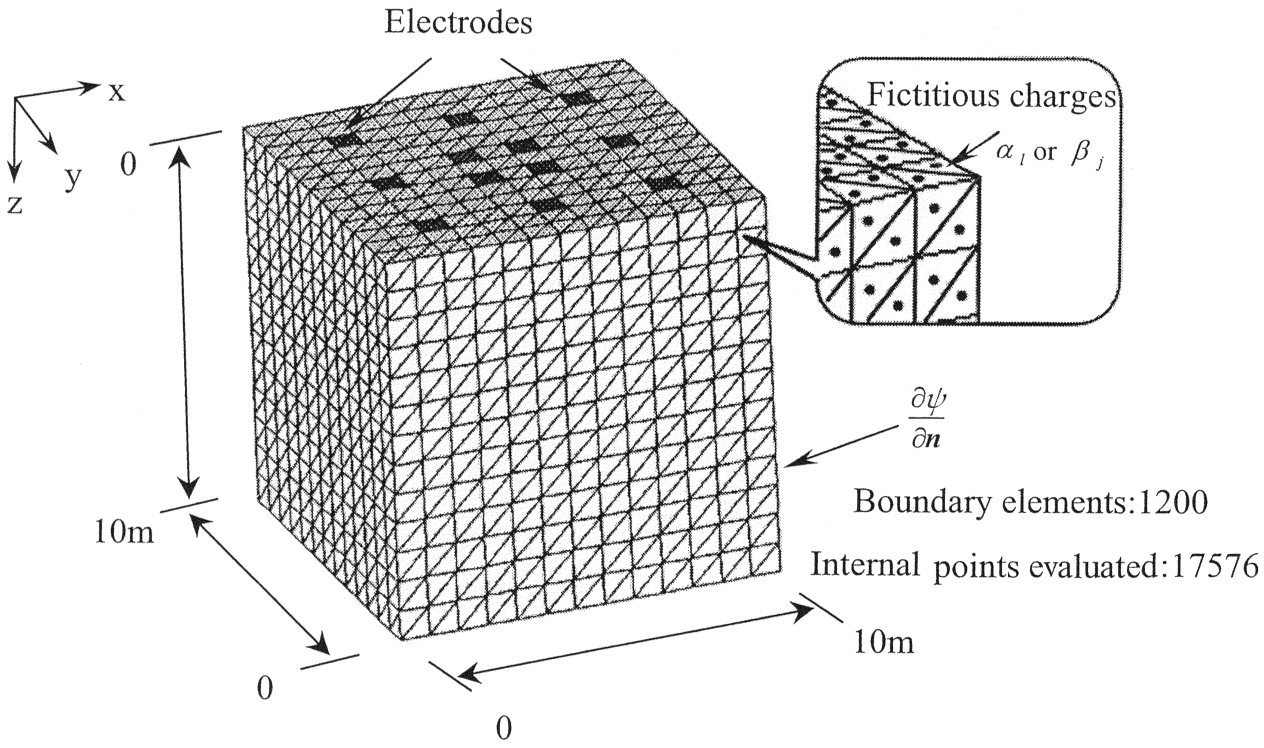

Fig. 2: 3D field with the electrodes on the surface

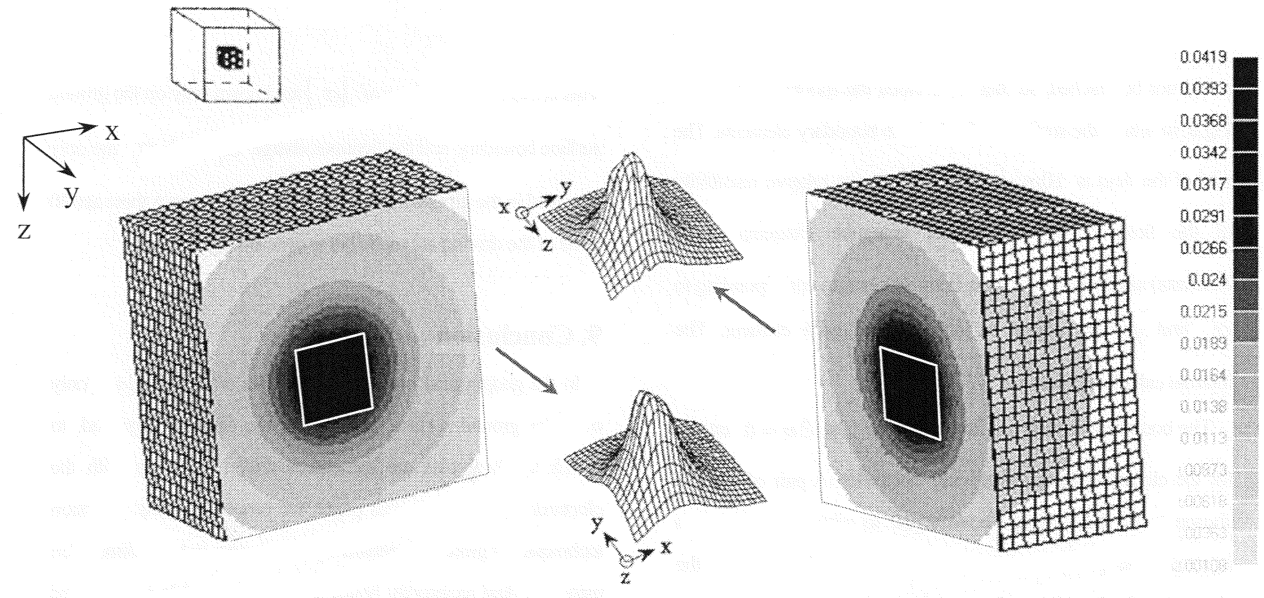

(a) An example of the original distribution and the potential changes (cut in the plane z=5.0, x=5.0)

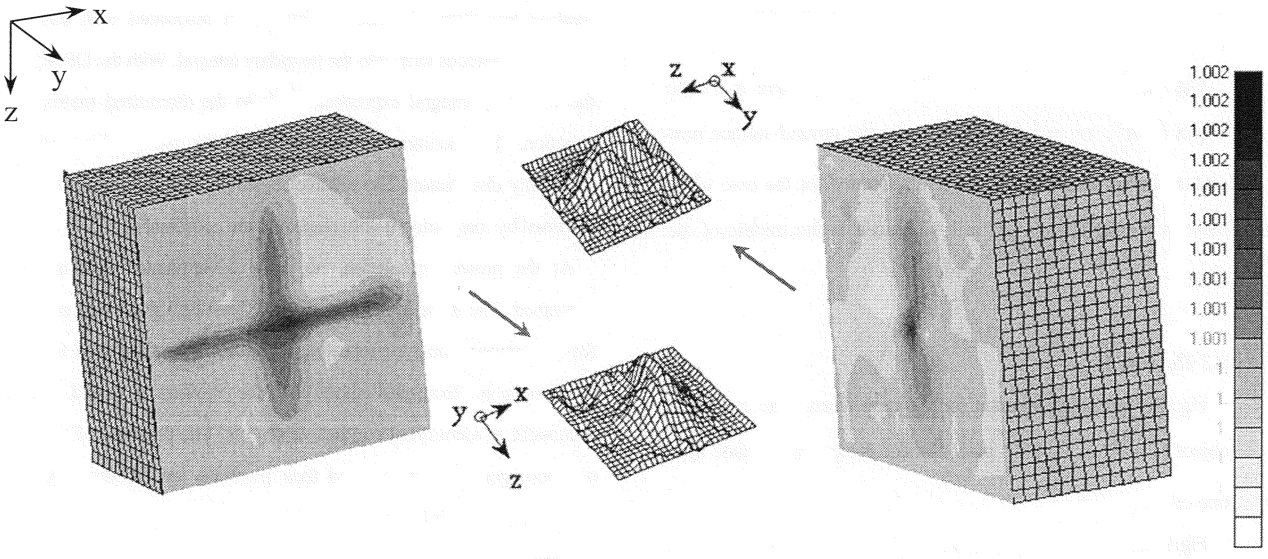

(b) The relative resisitivity distribution inverted (cut in the plane z=5.0, x=5.0)

Fig. 3: A cube object with the relative conductivity 10% higher, buried under the ground